Transactions of the 15th International Conference on
Structural Mechanics in Reactor Technology (SMiRT-15)
Seoul, Korea, August 15-20, 1999

Ultimate Limit State Design Check for Prestressed Concrete Shell

Umesh K. Rajeshirke and A. M. Kulkarni

STUP Consultants Limited, India

ABSTRACT: A large number of ducts are embedded in the containment shell for post-tensioning of prestressing cables. The pattern of stress/strains in the shell gets modified due to the presence of these voids. A method of analysis for ultimate limit state check for such shells is presented in this paper. The results of the study on the effect of voids on ultimate force carrying capacity of the section are discussed.

INTRODUCTION

To resist the membrane tensile stresses induced in containment shell in the event of postulated LOCA, the shell is generally prestressed by orthogonal sets of prestressing cables. Since the cables are post-tensioned, a large number of closely spaced ducts are embedded in the shell. Typical cross-sections are shown in Fig.1. The distribution of strains and stresses in the shell gets modified due to the presence of these voids.

Although numbers of methods are published in last couple of years on serviceability and ultimate limit state analysis of reinforced concrete shell element, the work is limited in the area of general shell i.e. with 'gross' sectional properties of shell (without presence of any voids). For the peculiar case of containment, it is necessary to study and evolve a procedure for design check of a cross-section of a prestressed concrete shell with large number of cable ducts, subjected to the membrane forces and bending moments. The same is presented in this paper.

MATERIAL PROPERTIES

Concrete

The parabolic-rectangular shaped compressive stress distribution diagram is shown in Fig.2. This is a typical design stress-strain curve referred in various codes like French BPEL-91, Eurocode-2 and Indian IS:456-1978. In this diagram the ultimate strain of concrete in compression is taken as $\varepsilon_{cu} = -0.35\%$, and the curve is defined by :

$$\sigma_c = \alpha f_{cd}\, 25(0.4+\varepsilon_c)\varepsilon_c \qquad \text{for } |\varepsilon_c| \leq 0.2\% \qquad (1)$$

and
$$\sigma_c = -\alpha f_{cd} \qquad \text{for } |\varepsilon_c| \geq 0.2\% \qquad (2)$$

In Eq.(1), ε_c should be introduced with negative sign i.e. ($\varepsilon_c \le 0$) and in %. The coefficient α is a reduction factor which allows for reduced compressive strength of concrete subjected over long period of time to high compressive stresses, and generally be assumed to be 0.80 or 0.85. γ_c is partial safety factor for concrete and to be taken as 1.5 for normal loading and 1.15 for accidental load conditions. The tensile stress in concrete is neglected.

Reinforcing Steel
A simplified stress strain diagram for reinforcing steel is shown in Fig.3. The partial safety factors for normal loading is taken as 1.15, and 1.0 for accidental load conditions.

Prestressing Steel
A simplified stress-strain diagram of prestressing steel is shown in Fig.4. A horizontal ideal-plastic branch with the stress $0.9\,f_{pk}/\gamma_s$ is considered with limits on $\Delta\varepsilon p$ equal to 2.0%, which is to be added to the strain $\varepsilon p^{(o)}$ corresponding to the pre-elongation of prestressing steel.

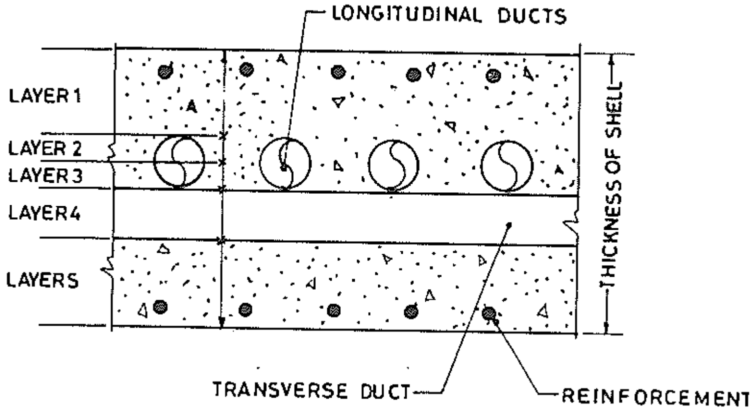

FIG.1
CROSS SECTION OF THE SHELL

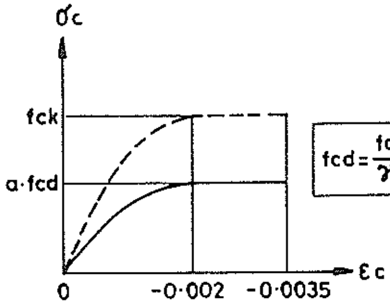

FIG. 2
PARABOLIC-RECTANGULAR STRESS-STRAIN DIAGRAM FOR CONCRETE

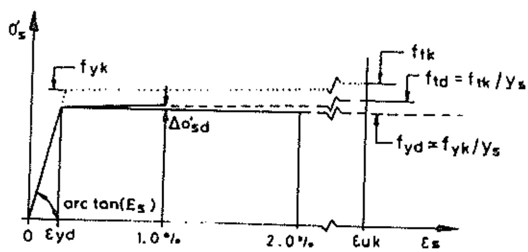

FIG.3
SIMPLIFIED STRESS-STRAIN DIAGRAMS FOR REINFORCING STEEL

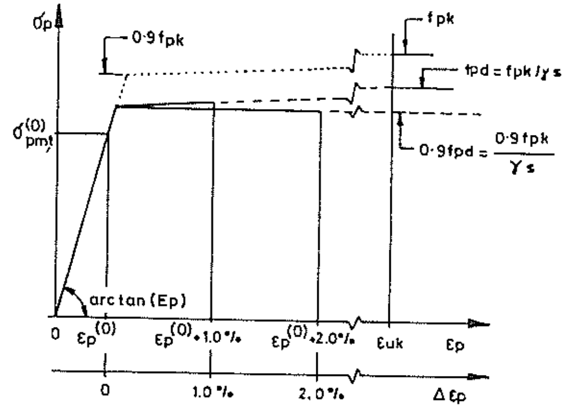

FIG.4

SIMPLIFIED STRESS-STRAIN DIAGRAMS FOR PRESTRESSING STEEL

STRAIN DIAGRAMS IN THE ULTIMATE LIMIT STATE

The possible strain diagrams in accordance with the stress-strain diagrams discussed above are shown in Fig.5. These diagrams are based on Bernoulli's hypothesis. The strain limits of the stress-strain diagram for concrete and steel result in five different domains for the design of cross-sections. With the assumption of the perfect bond, the strain diagrams in the Fig. 5 govern not only the concrete compressive stresses but also the stresses in reinforcement (reinforcing steel or prestressing steel including pre-strain $\varepsilon_p^{(o)}$ at any place in the cross section). The compressive strain of reinforcing steel caused by creep and shrinkage of concrete are normally negligible in ultimate limit state and hence not considered.

In domain 1, the whole section is subjected to uniform tensile strain whereas in domain-5, it is subjected to uniform compressive strain. In both the domains, the location of neutral axis is outside the section. The location of neutral axis changes from top fibre to bottom fibre of section in domain 2, 3 & 4. Similarly, the location of point 'C' (which is characterised by the compressive strain in concrete ε_c = 0.2%) also shifts from top to bottom in domains 2 to5 following the movement of neutral axis.

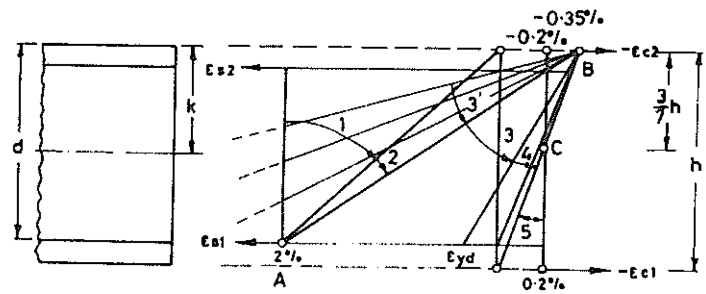

FIG. 5

STRAIN DISTRIBUTION FOR ULTIMATE LIMIT STATE

DESIGN CHECK

For a given cross-section, the ultimate force carrying capacity can be checked for uniform strain of -0.2%, if the applied membrane force is compressive, and for 2%, if the applied membrane force is tensile. The ultimate force carrying capacity of the section for given bending moment shall always be between these two limits. The position of neutral axis, for which the ultimate force carrying capacity of the section matches with the factored membrane force acting on the section is found out by solving the following equilibrium condition.

$$f(k) = Pus\ (k) + Puc\ (k) + N = 0 \tag{3}$$

Where N is the factored membrane force applied (sign conversion: compressive force positive)

Pus (k) and Puc(k) are the contributions from steel and concrete respectively in the ultimate resistance of the section and can be expressed as

$$Pus\ (k) = \Sigma\sigma_s(k)\ As. \tag{4}$$

and

$$Puc(k) = \int \sigma\ dAc. \tag{5}$$

The notation σ_s covers the steel stresses in both prestressed and non-prestressed steel.

After getting the location of neutral axis at equilibrium, the ultimate bending moment carrying capacity of the section about it is worked out and compared with the factored bending moment acting on the section.

Finding out the root of Eq.(3) involves solution of non-linear equation. The equation is solved numerically using Regula-falsi method. In this method, the initial assumptions of two values of k, one each on either side of solution are required. It is necessary to satisfy condition, i.e. $f(k_i) * f(k_{i+1}) < 0$ at each of iterations. A flow chart of the algorithm is shown in Fig. 6.

CONTRIBUTION FROM THE CONCRETE

The thickness of shell is divided into five different layers depending on the location of transverse and longitudinal ducts in the shell, as shown in Fig.1. The stresses in these layers may follow the rectangular or parabolic curve of compressive stress block of concrete depending on the position of neutral axis and consequently the position of point C in the thickness of the shell. If stresses in the layer are following rectangular part, their contribution to resisting membrane force is worked out easily by deducting the appropriate area of circular (due to longitudinal duct) or rectangular (due to transverse duct) voids from the gross area and then by multiplying by the uniform compressive stress. For a layer falling in parabolic stress zone (with strains less than 0.2%) the net contribution to resistance is worked out by deducting the contribution from the area of voids from the gross contribution of the section. To find out the deduction in resistance due to area of voids, the integration of stress is done numerically by dividing the portion of circular duct into many slices and averaging out the stresses over each slice.

NUMERICAL EXAMPLE

A cross-section of shell, having 500 mm thickness with 100 mm diameter ducts with spacing of 500 mm in transverse and longitudinal direction is analysed with and without considering the voids.

The characteristic strength of concrete considered is 40 MPa (Cube). Reinforcing steel, f_{yk} = 500 MPa and placed at 500mm^2/m, with effective cover of 50 mm is provided on inner and outer face. For simplicity, the contribution of prestressing steel to the ultimate resistance is not considered here, treating it as unbonded steel.

The section is analysed for various positions of neutral axis and corresponding ultimate force and moment carrying capacities of section are found out. The maximum ultimate compressive force carring capacity Pu_max and maximum moment carring capacity Mu_max for the section without considering voids are 10982.1 kN and 983.1 kN-m respectively.

Fig.7 shows the interaction diagram i.e. relation of ultimate membrane force Pu with corresponding ultimate moment carrying capacity Mu. The value Pu and Mu in the graph are normalised with respect to Pu_max and Mu_max respectively. The curves are plotted for both the cases, i.e. with and without considering the voids, for comparison.

SUMMARY

The effect on ultimate limit state design check considering voids due to the cable ducts embedded in prestress concrete shell of nuclear containment is discussed with numerical example. It is found that for a given example, the ultimate compressive force carrying capacity of the section (in absence of bending moment, shown as point P in fig. 7) reduces by 20 % when voids are considered. The difference is more significant for Pu/Pu_max greater than 0.34. However, there is no significant reduction in the ultimate moment carrying capacity of the section (in absence of membrane force acting, shown as point Q in fig. 7) even if the voids are considered in design check.

The method discussed here is useful for developing the design aids by varying the parameters like grades of concrete, thickness of shells, duct diameter and spacing.

REFERENCES

1. Concrete Structures, Euro Design Handbook, Ernest & Sohn, Berlin, 1995.
2. Regles BPEL-91, Regles Techniques De Conception Et De Calcul Des Ouvrages Et Constructions En Beton Precontraint Suivant la methode de etats limits.
3. BIS 456-1978 – Code of Practice for Plain and Reinforced Concrete (Third Revision).

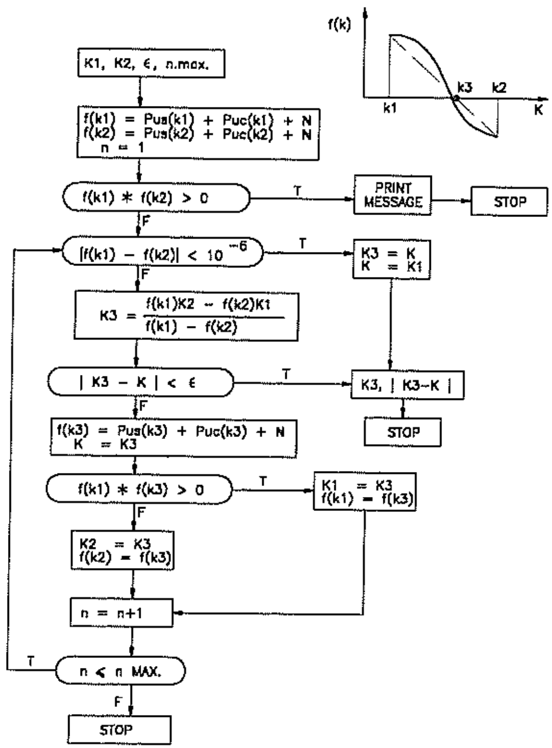

Fig. 6 : Flow Chart for Finding k at Equilibrium

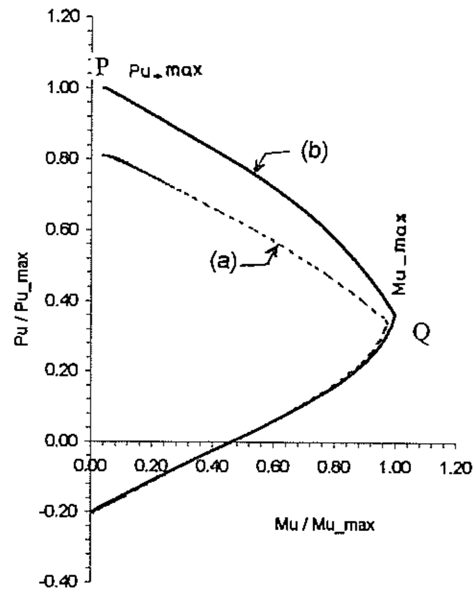

Fig.7 : Curve Showing Interaction of Ult. Memebrane Force with Ult. Bending Moment
(a) With Considering Voids
(b) Without Considering Voids